

**AIP** | Applied Physics
Letters

Optical determination of three-dimensional nanotrack profiles generated by single swift-heavy ion impacts in lithium niobate

J. Olivares, A. García-Navarro, G. García, A. Mýndez, and F. Agulló-López

Citation: *Appl. Phys. Lett.* **89**, 071923 (2006); doi: 10.1063/1.2236221

View online: <http://dx.doi.org/10.1063/1.2236221>

View Table of Contents: <http://apl.aip.org/resource/1/APPLAB/v89/i7>

Published by the [American Institute of Physics](http://www.aip.org).

Additional information on *Appl. Phys. Lett.*

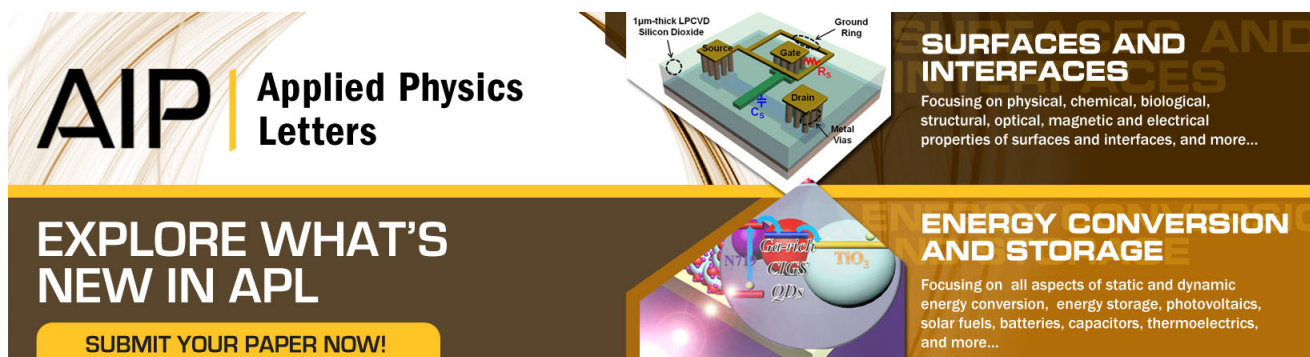
Journal Homepage: <http://apl.aip.org/>

Journal Information: http://apl.aip.org/about/about_the_journal

Top downloads: http://apl.aip.org/features/most_downloaded

Information for Authors: <http://apl.aip.org/authors>

ADVERTISEMENT



AIP | Applied Physics
Letters

**EXPLORE WHAT'S
NEW IN APL**

SUBMIT YOUR PAPER NOW!

SURFACES AND INTERFACES
Focusing on physical, chemical, biological, structural, optical, magnetic and electrical properties of surfaces and interfaces, and more...

ENERGY CONVERSION AND STORAGE
Focusing on all aspects of static and dynamic energy conversion, energy storage, photovoltaics, solar fuels, batteries, capacitors, thermoelectrics, and more...

Labels in diagrams: 1µm-thick LPCVD Silicon Dioxide, Source, Drain, Metal Vias, Ground Ring, QDs, CNTs, CIGS, NO₂.

Optical determination of three-dimensional nanotrack profiles generated by single swift-heavy ion impacts in lithium niobate

J. Olivares^{a)}

Instituto de Optica, CSIC, C/Serrano 121, 28006 Madrid, Spain

A. García-Navarro, G. García, A. Mýndez,^{b)} and F. Agulló-López^{b)}

Centro de Microanálisis de Materiales (CMAM), UAM, Cantoblanco, 28049 Madrid, Spain

(Received 3 March 2006; accepted 5 June 2006; published online 18 August 2006)

Three-dimensional (3D) profiles of single nanotracks generated by a low impact density of Cl ions at 46 MeV have been determined by optical methods, using an effective-medium approach. The buried location of the maximum stopping power induces a surface optical waveguiding layer even at ultralow fluences (10^{11} – 10^{13} at./cm²) that allows to obtain the effective refractive index profiles (from dark-mode measurements). Combining the optical information with Rutherford backscattering spectroscopy/channeling experiments, the existence of a surrounding defective halo around the amorphous track core has been ascertained. The 3D profile of the halo has also been determined. © 2006 American Institute of Physics. [DOI: 10.1063/1.2236221]

There is abundant evidence that swift-heavy ions, having energies ≥ 0.1 – 1 MeV/amu, generate, in many materials, amorphous tracks with nanometric radius along their trajectory^{1–6} when the electronic stopping power S_e is above a certain threshold S_{th} (~ 5 keV/nm for LiNbO₃). The radius of the track is a growing function of S_e and so it can be varied through the irradiation conditions. The peculiarity of track formation is that responsible mechanisms rely on electronic excitations and not on nuclear collision effects as in usual ion implantation experiments. The tracks can be selectively etched to produce nanochannels that, in turn, can be refilled with inorganic or organic substances having a number of promising applications.^{7,8} It is expected that in transparent crystals, e.g., LiNbO₃, the occurrence of amorphous tracks with a much lower refractive index than that of the surrounding crystalline material should have relevant implications on photonic performance, provided that control of morphology is achieved. Actually, in the track overlapping regime, an alternative route for the fabrication of good quality high-index jump optical waveguides⁹ has been demonstrated with fluences of $\sim 10^{14}$ – 10^{15} cm⁻², two orders of magnitude lower than with light-ion implantation.¹⁰

In this work we address the processing of LiNbO₃ by means of swift-heavy ions in the single-track (i.e., not overlapping) regime. The main purpose has been the usage of optical methods (waveguide dark-mode analysis) to learn about the depth morphology of the tracks and about the potential for tailoring the optical response of the irradiated region. One should stress that most techniques used to observe tracks cannot readily yield depth profiles, since they are either superficial^{11–13} or chemically aggressive¹⁴ or elaborate and difficult to interpret.¹⁵ In this letter the existence of a surrounding defective halo around the amorphous track core has been ascertained and the three-dimensional (3D) profile of the tracks has also been determined. The exciting prospect for photonic applications is that an effective (nanostructured)

waveguiding layer appears even for low enough fluences where ion tracks are well separated (~ 10 nm at 10^{12} at./cm²). This represents a breakthrough in the fluences required in comparison with standard implantation methods requiring fluences of $\sim 10^{16}$ – 10^{17} cm⁻², which adds to the intrinsic potential of the nanostructuring.

Congruent X-cut LiNbO₃ plates purchased from CASIX were irradiated at room temperature with Cl⁸⁺ ions at 45.8 MeV in the 5 MV tandem accelerator¹⁶ installed at the Center for Microanalysis of Materials (CMAM). Total fluences were in the range of 10^{11} – 10^{13} cm⁻². The optical characterization of the irradiated samples was made by means of the standard dark-mode technique by light coupling through a rutile prism. Light at 633 nm from a He–Ne laser with polarization control was used to determine both the ordinary and extraordinary refractive indices. In order to independently assess the area fraction that has become amorphized or disordered during irradiations, Rutherford backscattering spectroscopy (RBS)/channeling experiments along the *X* axis have been performed using 3 MeV H as probing ion. From the comparison of channeled and random spectra, the relative volume showing heavy disorder (as to destroy the channeling condition) has been determined.

The strategy of our method is illustrated in Fig. 1 where the stopping power $S_e(z)$ for Cl (46 MeV) calculated with SRIM2003 is plotted as a function of *z*, Fig. 1(a), together with a qualitative illustration of the (average) expected track profile, Fig. 1(b). As shown below in this letter, it includes a low-index amorphous core ($n_a=2.10$ at $\lambda=633$ nm) and a defective surrounding halo. Following the $S_e(z)$ curve, the track radius should increase with depth up to a maximum and then decrease with increasing *z*. In Fig. 1(a) the dotted line shows the predicted (“amorphization”) threshold according to recent data¹⁷ that include the effect of ion velocity. The measured ordinary and extraordinary refractive index profiles, $n_o(z)$ and $n_e(z)$, induced by the Cl (46 MeV) irradiations are shown in Figs. 2(a) and 2(b), respectively. They can be well described by a third-order polynomial that, as expected from the low impact densities, scales linearly with the ion fluence within experimental error. This allows for a meaningful extrapolation of the refractive index profiles

^{a)} Author to whom correspondence should be addressed; electronic mail: j.olivares@io.cfmac.csic.es

^{b)} Also at Departamento de Física de Materiales, UAM, Cantoblanco, 28049 Madrid, Spain.

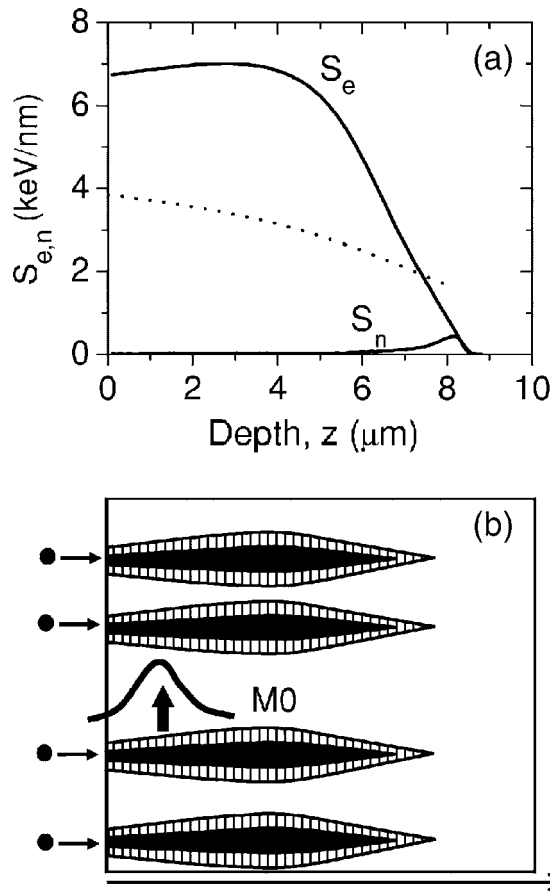


FIG. 1. (a) Electronic, S_e , and nuclear, S_n , stopping power curves for Cl 45.8 MeV in LiNbO₃ calculated with SRIM2003. The dotted line shows the corresponding “amorphization” threshold curve from the data collected in Ref. 17. (b) Schematic depth morphology of the tracks, showing the core (black) and the surrounding halo (dashed). An schematic light profile (MO) illustrates waveguiding behavior.

down to the lowest fluences [$(1-2) \times 10^{12} \text{ cm}^{-2}$] where only one or two guided modes are measured. Note how on increasing fluence the refractive indices decrease towards the minimum saturation value ($n_a=2.10$) corresponding to the isotropic amorphous phase achieved by full track overlapping.^{9,18}

Assuming that every ion impact has produced an identical track, one could readily obtain the amorphized fraction and so the radius R_c of the track core (area $\sigma_c = \pi R_c^2$) as a function of z , by averaging the dielectric constants for the core and bulk crystal. Remarkably, these calculations give quite different values for the amorphized (core) fraction depending on whether the ordinary or extraordinary profiles are used. This discrepancy suggests that one should take into account the existence of a third birefringent optical medium i.e., a surrounding defective halo with outside radius R_h and area $\sigma_h = \pi(R_h^2 - R_c^2)$. The occurrence of a heavily damaged halo has been inferred in other materials from transmission electron microscopy observations¹² and consists of strained or defective material¹⁹ that should have refractive indices different from those of the bulk crystal. Consequently, one should write the simple averaging equations for the dielectric constants $\epsilon = n^2$,

$$\bar{n}_o^2 = n_o^2 + f_a(n_a^2 - n_o^2) + f_h \langle \Delta n_o^2 \rangle, \quad (1a)$$

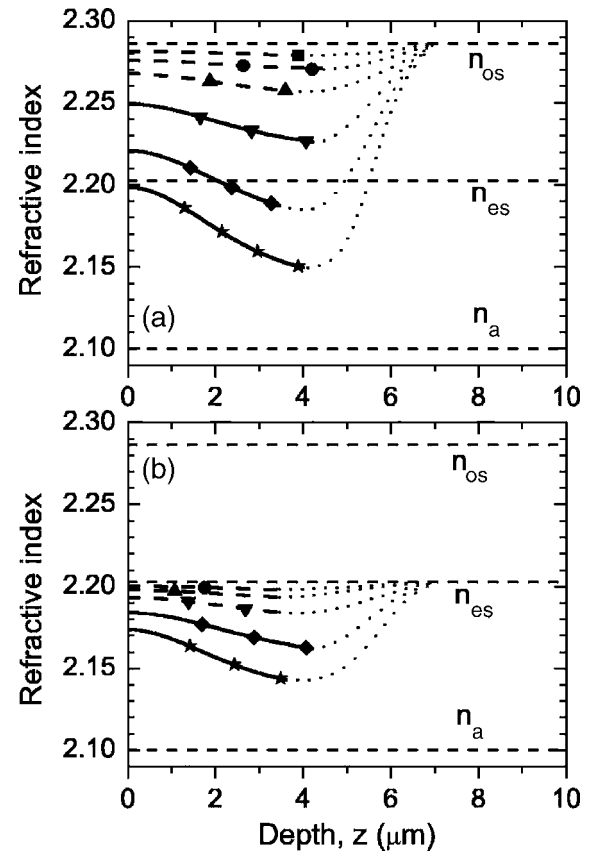


FIG. 2. Ordinary (a) and extraordinary (b) refractive index profiles (solid lines) at $\lambda=633 \text{ nm}$ for X-cut LiNbO₃ samples irradiated with Cl 45.8 MeV ions at the fluences (at./cm²) of 5×10^{11} (squares), 1×10^{12} (circles), 2×10^{12} (up triangles), 4×10^{12} (inverted triangles), 8×10^{12} (rhombi), and 1×10^{13} (stars). Horizontal dashed lines show the refractive index values for the crystal (n_{os} and n_{es}) and amorphous (n_a) regions. A guess of the expected refractive index profiles behind the minimum is also plotted with a dotted line.

$$\bar{n}_e^2 = n_e^2 + f_a(n_a^2 - n_e^2) + f_h \langle \Delta n_e^2 \rangle, \quad (1b)$$

where $\langle \Delta n_{o,e}^2 \rangle \cong 2n_{o,e} \langle \Delta n_{o,e} \rangle$ is the change in the average dielectric constants of the halo in comparison to the crystal host. f_a and f_h are, respectively, the total amorphous (core) and damaged (halo) fractions such that $f_a + f_h + f_v = 1$ (f_v being the fraction of the remaining virgin crystal). In order to solve Eq. (1) and obtain f_a and f_h , additional information is required. For example, it is well documented for LiNbO₃ that during the first stages of damaging, the extraordinary refractive index increases whereas the ordinary index decreases¹⁰ and that the relation $n_e \Delta n_e \approx -2n_o \Delta n_o$ ($\Delta n_e > 0, \Delta n_o < 0$) is approximately obeyed. This has been also confirmed in experiments below the amorphization threshold at the surface where only the halo (and not the core) is generated.⁹

With the above assumption, $n_e \langle \Delta n_e \rangle = -2n_o \langle \Delta n_o \rangle$, one can now solve Eqs. (1) for $f_a(\phi)$ at the crystal surface (ϕ being the ion fluence) illustrated in Fig. 3. One confirms that the fraction of the area covered by the core is essentially proportional to fluence. The corresponding average value $R_c(z)$ caused by a single impact has been determined and is plotted in Fig. 4. The track radius shows a clear increase with depth in correlation with the shape of the $S_e(z)$ curve in the surface region. One can now compare these profiles with data recently reported¹⁷ for the track radii at the surface of LiNbO₃. In our case (ion energy slightly above

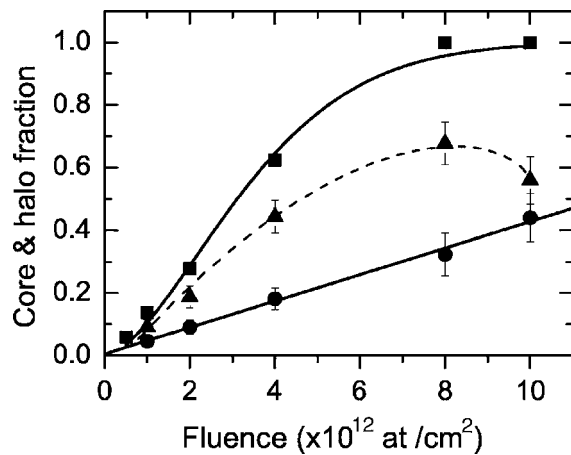


FIG. 3. Core (amorphous) fraction f_a at the surface (circles) and the corresponding linear fit. Total disordered fraction f_d (squares), the solid line is a fit to an Avrami formula with $n=1.6$. The difference between the total disordered and core fractions is the halo fraction (triangles). The dashed line is a guide for the eye.

1 MeV/amu), the expected radius at the surface was in the 1–2 nm range in accordance with our optical method.

In order to proceed with our analysis, it is useful to complement the optical information for $f_a = \phi\pi R_c^2$ with the total “disordered” fraction f_d obtained from RBS/channeling spectra. How are these two fractions compared? The disordered fraction at the surface is derived through the equation

$$f_d = \frac{Y_{ch}(\phi) - Y_{ch}(0)}{Y_r - Y_{ch}(0)}, \quad (2)$$

where Y_r and Y_{ch} are, respectively, the random and channeled incidence RBS yields. Dechanneling effects during ion propagation have been taken into account through a simple phenomenological model.²⁰ The f_d data, included in Fig. 3, show a much more extensive disorder than that corresponding to the amorphous core deduced from the optical data. This appears reasonable since channeling is very sensitive to lattice distortions and should also “see” the halo surrounding the latent track. Therefore, one should write $f_d(\text{RBS}) = f_a(\text{optical}) + f_h$, and so the fraction $f_h(\phi)$ covered by the halos (also included in Fig. 3) as well as their average area σ_h and outside radius R_h can be easily calculated (see Fig. 4). Note that at the sample surface, R_h is about twice R_c . As a final point one should note the saturation effects associated to track overlapping in the $f_d(\phi)$ curve at variance with the behavior of the core fraction. In fact, the data depart from a purely Poisson law and fit an Avrami dependence $f_d = 1 - \exp[-(\phi/\phi_c)^n]$, with exponent $n=1.6$ suggesting some interaction between halos.

In summary, the 3D profiles of the nanotracks caused by single swift-heavy ion impacts (Cl 46 MeV) in LiNbO₃ have been determined down to a depth of $\approx 3.5 \mu\text{m}$ by combining optical (waveguide dark modes) and RBS/channeling methods. It has been found that tracks are composed of an amorphous core surrounded by a damaged halo. The measured radius of the track core at the surface shows a reasonable accordance with previously reported data. This work should help pave the way for the fabrication and characterization of

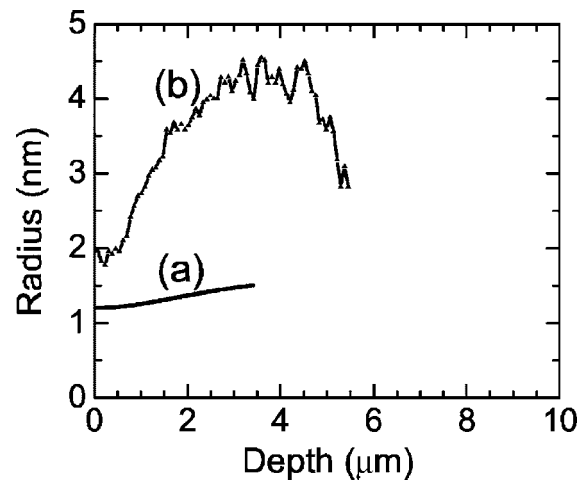


FIG. 4. Depth dependence of the core radius (a) and of the core plus halo radius (b).

nanostructured photonic devices by means of irradiation with swift-heavy ions with ultralow fluences.

The authors acknowledge funding from project No. GR/MAT/0514/2004 from the regional government CAM. One of the authors (A.G.-N.) acknowledges the financial support of the MEC through a FPU fellowship and of the Madrid City Council in the Residencia de Estudiantes.

- ¹R. Spohr, in *Ion Tracks and Microtechnology: Basic Principles and Applications*, edited by K. Bethge (Vieweg, Braunschweig, 1990).
- ²P. Hansen and H. Heitmann, *Phys. Rev. Lett.* **43**, 1444 (1979).
- ³B. Canut, A. Benyagoub, G. Marest, A. Meftah, N. Moncoffre, S. M. M. Ramos, P. Studer, P. Thevenard, and M. Toulemonde, *Phys. Rev. B* **51**, 12194 (1995).
- ⁴C. Trautmann, M. Toulemonde, J. M. Constantini, J. J. Grob, and K. Schwartz, *Phys. Rev. B* **62**, 13 (2000).
- ⁵A. Benyagoub, F. Levesque, F. Couvreur, C. Gibert-Mougel, C. Dufour, and E. Paumier, *Appl. Phys. Lett.* **77**, 3197 (2000).
- ⁶P. I. Gaiduk, A. Nylansted-Larsen, J. Lundsgaard-Hansen, C. Trautmann, and M. Toulemonde, *Appl. Phys. Lett.* **83**, 1746 (2003).
- ⁷M. Toulemonde, C. Trautmann, E. Balanzat, K. Hjort, and A. Weidinger, *Nucl. Instrum. Methods Phys. Res. B* **216**, 1 (2004).
- ⁸J.-H. Zollondz and A. Weidinger, *Nucl. Instrum. Methods Phys. Res. B* **225**, 178 (2004).
- ⁹J. Olivares, G. García, A. García-Navarro, F. Agulló-López, O. Caballero, and A. García-Cabañes, *Appl. Phys. Lett.* **86**, 183501 (2005).
- ¹⁰P. D. Townsend, P. J. Chandler, and L. Zhang, *Optical Effects of Ion Implantation* (Cambridge University Press, London, 1994).
- ¹¹F. Thibaudau, J. Cousty, E. Balanzat, and S. Bouffard, *Phys. Rev. Lett.* **67**, 1582 (1991).
- ¹²J. Vetter, R. Scholz, and N. Angert, *Nucl. Instrum. Methods Phys. Res. B* **91**, 129 (1994).
- ¹³J. Ackermann, N. Angert, R. Neumann, C. Trautmann, M. Dischner, T. Hagen, and M. Sedlacek, *Nucl. Instrum. Methods Phys. Res. B* **107**, 181 (1996).
- ¹⁴K. Schwartz, *Nucl. Instrum. Methods Phys. Res. B* **107**, 128 (1996).
- ¹⁵D. Albrecht, P. Armbruster, R. Spohr, M. Roth, K. Schaubert, and H. Stuhmann, *Appl. Phys. A: Solids Surf.* **37**, 37 (1985).
- ¹⁶www.uam.es/cmam
- ¹⁷A. Meftah, J. M. Costantini, N. Khalfou, S. Boudjadar, J. P. Soquert, F. Studer, and M. Toulemonde, *Nucl. Instrum. Methods Phys. Res. B* **237**, 563 (2005).
- ¹⁸J. Olivares, G. García, F. Agulló-López, F. Agulló-Rueda, A. Kling, and J. C. Soares, *Appl. Phys. A: Mater. Sci. Process.* **A81**, 1465 (2005).
- ¹⁹F. Agulló-López, G. García, and J. Olivares, *J. Appl. Phys.* **97**, 093514 (2005).
- ²⁰*Handbook of Modern Ion Beam Materials Analysis*, edited by J. R. Tesmer and M. Nastasi (MRS, Pittsburgh, 1995).